REPORT

AD-A267 886

Form Approved OBM No. 0704-0188

1. Agency Use Only (Leave blank) | January 1993 | ...pe and Dates Covered. Final - Journal Article

4. Title and Subtitle.
A Three-way Comparison of Sea Level from the Central Equatorial Pacific, 1985-89

5. Funding Numbers.
Program Element No. 0601153N
Project No. 3105
Task No. 330
Accession No. DN258028
Work Unit No. 13232J

6. Author(s).
Xiaoli Zhu*, Mark Wimbush*, Kathleen A. Donohue*, Stephen M. Chriswell**, Roger Lukas***, Laury Miller****, and Harley E. Hurlburt

7. Performing Organization Name(s) and Address(es).
Naval Research Laboratory
Oceanography Division
Stennis Space Center, MS 39529-5004

8. Performing Organization Report Number.
JA 323:101:92

9. Sponsoring/Monitoring Agency Name(s) and Address(es).
Naval Research Laboratory
Oceanography Division
Stennis Space Center, MS 39529-5004

10. Sponsoring/Monitoring Agency Report Number.
JA 323:101:92

11. Supplementary Notes.
Published in TOGA Notes.
*Univ. of Rhode Island, **New Zealand Oceanographic Institute, Wellington, New Zealand, ***Univ. of Hawaii, ****NOAA/NOS Geosciences Lab, Rockville, MD

12a. Distribution/Availability Statement.
Approved for public release; distribution is unlimited.

12b. Distribution Code.

13. Abstract *(Maximum 200 words).*

Temporal and spatial features of central equatorial Pacific Ocean sea-level variation appear similar, in measurements from two very different systems (one in the ocean and one carried on a satellite), and in results from a numerical model of the region. In particular, there is an interannual cycle: during El Nino, Kelvin waves appear at the equator, and the sea surface ridge associated with the equatorial current system shifts southward; in non El Nino years, instability waves appear at 69°N, and the ridge shifts to the north. This three-way comparison gives support both to measurement systems and to the numerical model.

93-17941

14. Subject Terms.
Ocean models, ocean forecasting, fronts (oceanography)

15. Number of Pages.
4

16. Price Code.

17. Security Classification of Report.	18. Security Classification of This Page.	19. Security Classification of Abstract.	20. Limitation of Abstract.
Unclassified	Unclassified	Unclassified	SAR

NSN 7540-01-280-5500

Standard Form 298 (Rev. 2-89)
Prescribed by ANSI Std. Z39-18
298-102

93 8 4 213

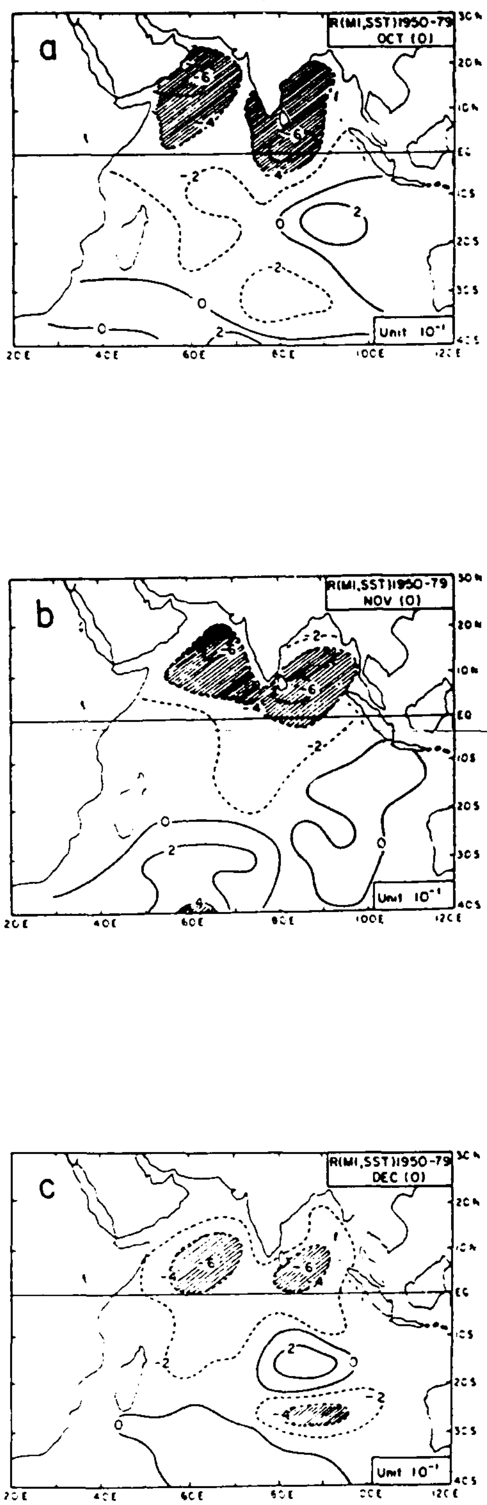

Figure 3. Same as Figure 1, except for the months after the monsoon.

A Three-way Comparison of Sea Level from the Central Equatorial Pacific, 1985-89

Introduction

Temporal and spatial features of central equatorial Pacific Ocean sea-level variation appear similar, in measurements from two very different systems (one in the ocean and one carried on a satellite), and in results from a numerical model of the region. In particular, there is an interannual cycle: during El Niño, Kelvin waves appear at the equator, and the sea-surface ridge associated with the equatorial current system shifts southward; in non-El Niño years, instability waves appear at 6°N, and the ridge shifts to the north. This three-way comparison gives support both to measurement systems and to the numerical model.

In Situ and Satellite Measurements and a Numerical Model

Coincidentally, from early 1985 until late 1989 there were two quite different instrument systems recording sea level across the central equatorial Pacific Ocean. One was an *in situ* array of inverted echo sounders (Chaplin and Watts, 1984), island subsurface-pressure gauges, and sea-level gauges, maintained near 160°W. The other was the Geosat altimeter. We consider the records from these two systems, comparing them with one another and with the output of a 3½-layer numerical model of the global ocean. During the five-year duration of this three-way intercomparison, there occurred a warm El Niño event in 1986-87 and a cold La Niña event in 1988-89.

The *in situ* array contained three inverted echo sounders at 10°N, 8°N, and 6°N, and island subsurface-pressure or sea-level gauges at 6°N, 4°N, 2°N, 0.4°S, 4°S, and 9°S. Since the array has ~2° spacing only between 10°N and near the equator, we consider here only data at stations in this interval. The longitudes of these stations ranged from 157.5°W to 162.5°W. The data were processed and converted to sea level (or equivalently dynamic height), as described in Wimbush *et al.* (1990). Data gaps of ~1 year each at 8°N (1986-87) and 10°N (1988-89) were appropriately patched (Donohue *et al.*, 1992).

The Geosat time series were computed using a combination of crossover and collinear methods (Miller and Cheney, 1990). After applying the standard corrections provided in the Geosat geophysical data records (Cheney *et al.*, 1991a,b), the geodetic mission data were processed into crossover differences and the exact repeat mission data were processed into collinear differences, to remove all time-invariant signals. Subsequently, a linear trend was removed from the differences along each satellite arc over the range 40°S-40°N to eliminate time-varying orbit error, and the results were binned in areas 8° in longitude by 1° in latitude. The sample interval in a typical 8° x 1° area is approximately 2 days for both types of data. After performing a least-squares adjustment to the crossover data and shifting the collinear data to have the same mean as the crossover data in a 1-year overlap, the combined data were low-pass filtered, with half-power periods 95 and 30 days, to produce data sets for analysis with two different degrees of smoothness.

Means of both the *in situ* and altimeter time series at each latitude were set to match 0-2000 db dynamic heights calculated, for these latitudes, from mean climatology (Levitus, 1982) averaged over the longitude range of the array.

The 3½-layer global ocean model is a descendent of a model by Hurlburt and Thompson (1980), with extended capability (Wallcraft, 1991). The horizontal resolution is 0.35° in longitude and 0.25° in latitude. The model was spun up from rest to statistical equilibrium using the Hellerman and Rosenstein (1983) monthly wind stress climatology, then integrated from 1981 to 1991 using monthly averaged European Centre for Medium-range Weather Forecasting 1000 mb winds with the 1981-91 mean replaced by the Hellerman-Rosenstein annual mean. The model is thermodynamic (prognostic density equation) to allow varying stratification, but the only thermal forcing is a relaxation to the annual mean density climatology (Levitus, 1982). Additional results from this simulation can be found in Metzger *et al.* (1992). For our comparison, time series of model sea surface height were sampled at 0.1-month intervals. These time series cover 0.5°S to 10°N at 0.5° intervals along 160°W.

Intercomparison of Results

Figure 1 shows plots of all three time-series sets contoured in time-latitude space.

In this figure, the *in situ* and model output time series have been low-pass filtered in visual accord with the smoothness of the Geosat data set. The *in situ* data, Geosat data, and model output all show the following features. The height of the zonal sea-surface ridge (Wyrtki, 1974) associated with the North Equatorial Countercurrent varies seasonally, typically being maximum in October and minimum in April. From the ridge to the trough (usually near 4°N and 10°N, respectively), the height difference has an October maximum of about 25 cm. From year to year, the position of the ridge varies: it is farthest south (~2°N) during the warm event (principally in 1986), and farthest north (~6°N) during the cold event (in 1988). Also, at the very end of 1989, after the Geosat data end, there is another northward movement of the ridge to 6°N visible in both the *in situ* data and the model output.

Complex demodulation amplitudes (Koopmans, 1974) were computed and averaged over the 1985-89 duration of the time series. In Figure 2 these average amplitudes are contoured as functions of period and latitude. Note, in all three cases, the two high-amplitude peaks at about 6°N.

The *in situ* data show these two peaks at periods of 45 days and 1 year. The 45-day peak is probably an equatorial current system instability (Philander *et al.*, 1985), a westward extension of waves originally seen in satellite thermal images of the eastern equatorial Pacific (Legeckis, 1977). The annual oscillation has a node near 8°N and another peak to the north of 10°N, but with the opposite phase (see Figure 1). There is yet another slight peak, at 80 days period, centered on the equator and extending out to about 3° latitude, consistent with the form of an equatorial Kelvin wave (Fu *et al.*, 1991). Looking at these amplitudes year by year (not shown), it is apparent that during the 1986-87 warm event, this Kelvin-wave peak is especially strong while the instability-wave peak is absent. Also the instability-wave peak period varies from year to year, being shortest during the 1988-89 cold event. In a plot similar to Figure 1a, but of unfiltered data (not shown), it is clear that these waves are strongest near year's end, and essentially absent in spring when ridge height is a minimum and consequently the current system is weakest.

The Geosat data show the same general spectral and spatial character: the annual peak has a very similar latitudinal structure, the instability-wave peak is again near 6°N, and a Kelvin-wave peak appears at 80 days period. There is an additional peak at about 100 days period near 8°N. A similar peak at 9°N in the eastern Pacific has been previously observed with inverted echo sounders (Miller *et al.*, 1985). Looking at the Geosat amplitudes year by year (not shown), the peak appears at 8°N during the 1986-87 warm event, the time of the *in situ* data gap at this latitude. Hence, though not visible in our *in situ* data, this peak, of unknown origin, is probably real nevertheless.

The numerical model output shows the same general features as the *in situ* and Geosat data sets, except the equatorial Kelvin-wave peak and 8-9°N peak are not visible. The instability-wave peak here has a longer period (70 days) and is centered at 6.5°N. Absence of the Kelvin peak and shifting of the instability wave toward longer periods may be results of the monthly averaging of the wind-field input.

While there are differences in the details, it is encouraging to see broad agreement in several fundamental characteristics of these time series from very different sources. Of particular interest are the El Niño cycle variation of the high-pressure-

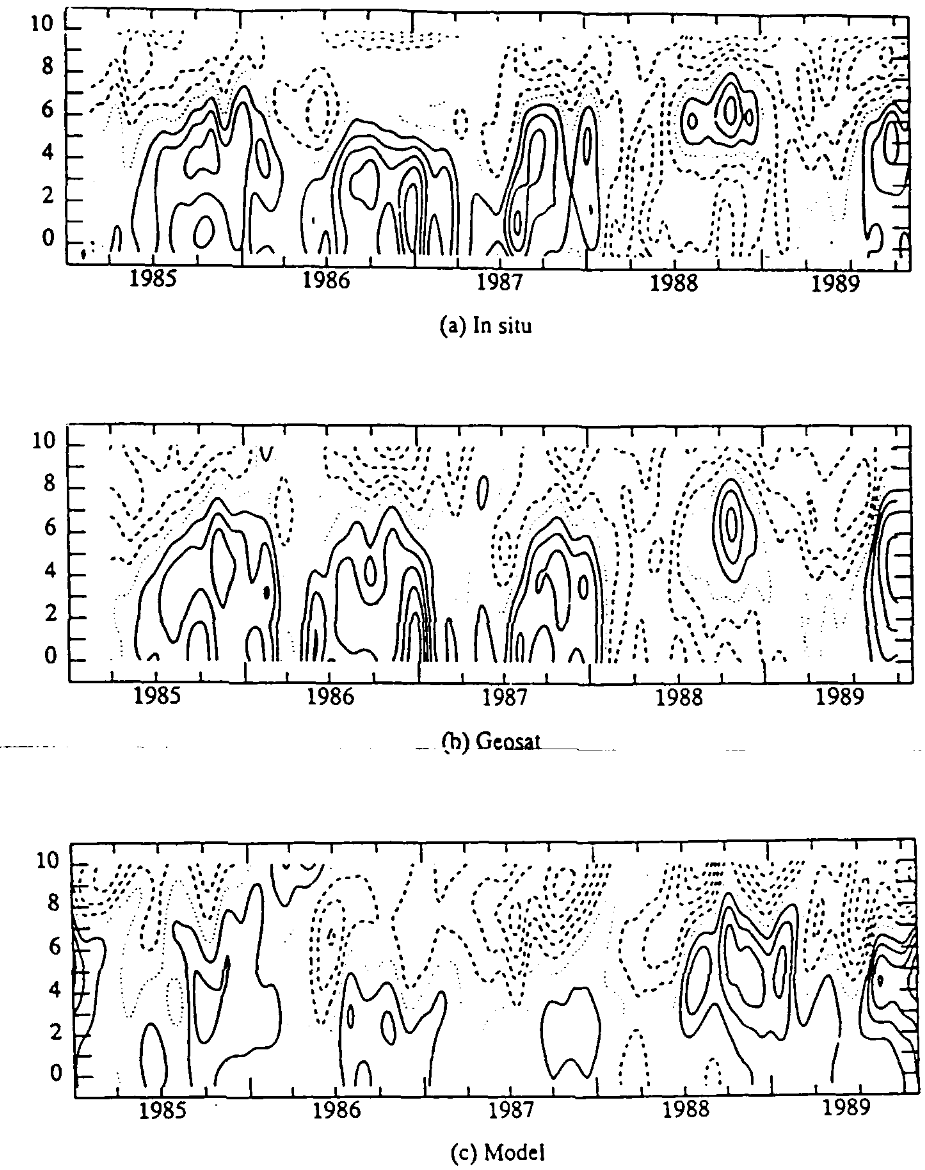

Figure 1. Sea surface elevation for the time period 1985-89, for (a) in situ *data (60-day low-pass filtered), (b) Geosat data (95-day low-pass filtered), (c) model output (30-day low-pass filtered). In each case, elevation is contoured as a function of time and northern latitude (in degrees). Contour interval is 5 cm. Positive, zero, and negative elevations are shown as solid, dotted, and dashed lines, respectively.*

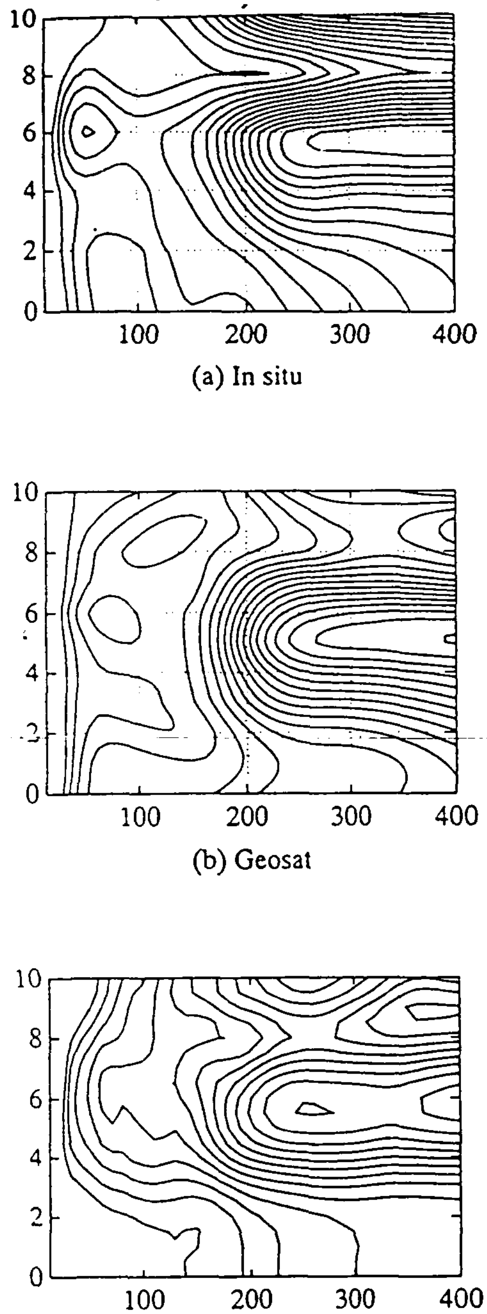

(a) In situ

(b) Geosat

(c) Model

Figure 2. Complex demodulation amplitudes of sea level averaged over the time period 1985-89 (except for a few missing weeks at the beginning of 1985 and the end of 1989 in (a) and (b)--see Figure 1), for (a) in situ *data, (b) Geosat data (30-day low-pass filtered), (c) model output. In each case, amplitude is contoured as a function of period (in days) and northern latitude (in degrees). The lowest-level contour shown is 2.5 cm and is the left-most contour in each panel. Contour interval is 0.5 cm.*

ridge latitude, and the 6°N instability-wave peak. In satellite infra-red images, this instability is clearly visible to the east as a wave-like disturbance of the thermal front near 2°N (Legeckis, 1977; Miller *et al.*, 1985).

From the data presented here, the pressure field perturbation associated with the instability appears greatest near 6°N. This is farther from the equator than (a) the instability's frontal expression, (b) pressure maxima of available low-meridional-mode, free equatorial waves (Fu *et al.*, 1991), (c) regions in which small-amplitude perturbations of the mean flow are barotropically unstable (Lukas, 1987; Luther and Johnson, 1990), and (d) latitudes of high eddy kinetic energy production (Luther and Johnson, 1990), all four of these being within 4° of the equator. But a maximum in eddy potential energy production in the thermocline (90 m depth) at about 7°N (Luther and Johnson, 1990) suggests a baroclinic instability in the North Equatorial Countercurrent, which may be responsible for the peak that we see. This instability-wave peak is not visible in Mitchum and Lukas's (1987) composite Pacific sea-level spectrum, because there were no measurements in the range 4-7°N. Nevertheless, it has been noted previously in Geosat data (Perigaud, 1990). We believe that reproduction of these features is an important measure of success for equatorial models.

Acknowledgments

This research was supported by the National Science Foundation, National Oceanic and Atmospheric Administration, Office of Naval Research, and Office of Naval Technology.

References

Chaplin, G.F., and D.R. Watts, 1984: Inverted echo sounder development. In *Oceans '84 IEEE-MTS Conf. Proc.*

Cheney, R.E., B.C. Douglas, and R.W. Agreen, 1991a: *Geosat Crossover Difference Handbook*, NOAA Manual NOS/NGS 6, National Ocean Service.

Cheney, R.E., W.J. Emery, B.J. Haines, and F. Wentz, 1991b: Recent improvements in Geosat altimeter data. *EOS*, 72, 577-580.

Donohue, K.A., M. Wimbush, S.M. Chiswell, and R. Lukas, 1992: *Line Islands Array 1985-1989 Data Report: Dynamic Height Time Series.* Graduate School of Oceanography Technical Report 92-5, University of Rhode Island, Narragansett, RI.

Fu, L.-L., J. Vazquez, and C. Perigaud, 1991: Fitting dynamic models to the Geosat sea level observations in the tropical Pacific Ocean. Part I: A free wave model. *J. Phys. Oceanogr.*, 21, 798-809.

Hellerman, S., and M. Rosenstein, 1983: Normal monthly windstress over the world ocean with error estimates. *J. Phys. Oceanogr.*, 13, 1093-1104.

Hurlburt, H.E., and J.D. Thompson, 1980: A numerical study of Loop Current intrusions and eddy shedding. *J. Phys. Oceanogr.*, 10, 1611-1651.

Koopmans, L.H., 1974: *The Spectral Analysis of Time Series.* Academic Press, New York.

Legeckis, R., 1977: Long waves in the eastern equatorial Pacific Ocean--a view from a geostationary satellite. *Science*, 197, 1179-1881.

Levitus, S., 1982: *Climatological Atlas of the World Ocean.* NOAA Professional Paper No. 13.

Lukas, R., 1987: Horizontal Reynolds stresses in the central equatorial Pacific. *J. Geophys. Res.*, 92, 9453-9463.

Luther, D.S., and E.S. Johnson, 1990: Eddy energetics in the upper equatorial Pacific during the Hawaii-to-Tahiti Shuttle Experiment. *J. Phys. Oceanogr.*, 20, 913-944.

Metzger, E.J., H.E. Hurlburt, J.C. Kindle, Z. Sirkes, and J.M. Pringle, 1992: Hindcasting of wind-driven anomalies using a reduced-gravity global ocean model. *J. Mar. Technol. Soc.*, 26, 23-32.

Miller, L., D.R. Watts, and M. Wimbush, 1985: Oscillations of dynamic topography in the eastern equatorial Pacific. *J. Phys. Oceanogr.*, 15, 1759-1770.

Miller, L., and R. Cheney, 1990: Large-scale meridional transport in the tropical Pacific during the 1986-87 El Niño from Geosat. *J. Geophys. Res.*, 95, 17905-17919.

Mitchum, G., and R. Lukas, 1987: The latitude-frequency structure of Pacific sea level variance. *J. Phys. Oceanogr.*, 17, 2362-2365.

Perigaud, C., 1990: Sea level oscillations observed with Geosat along the two shear fronts of the Pacific North Equatorial Countercurrent. *J. Geophys. Res.*, 95, 7239-7248.

Philander, G., D. Halpern, D. Hansen, R. Legeckis, L. Miller, C. Paul, R. Watts, R. Weisberg, and M. Wimbush, 1985:

Long waves in the equatorial Pacific Ocean. *EOS*, 66, 154-155.
Wallcraft, A., 1991: *The Navy Layered Ocean Model Users Guide*. NOARL Report No. 35, Stennis Space Center, MS.
Wimbush, M., S.M. Chiswell, R. Lukas, and K.A. Donohue, 1990: Inverted echo sounder measurement of dynamic height through an ENSO cycle in the central equatorial Pacific. *IEEE J. Oceanic Eng.*, 15, 380-383.
Wyrtki, K., 1974: Sea level and seasonal fluctuations of the equatorial currents in the western Pacific Ocean. *J. Phys. Oceanogr.*, 4, 91-103.

Xiaoli Zhu, Mark Wimbush, and Kathleen A. Donohue
Graduate School of Oceanography
University of Rhode Island
Narragansett, RI 02882, U.S.A.

Stephen M. Chiswell and Roger Lukas*
JIMAR, University of Hawaii
1000 Pope Road
Honolulu, HI 96822, U.S.A.

Laury Miller
NOAA/NOS Geosciences Lab, N/OES11
6001 Executive Boulevard
Rockville, MD 20852, U.S.A.

Harley E. Hurlburt
Naval Research Laboratory, Code 7323
Stennis Space Center, MS 39529, U.S.A.

**Present address:*
New Zealand Oceanographic Institute, NIWAR
P.O. Box 14-901, Kilbirnie
Wellington, New Zealand

Dissipation in a Pacific Equatorial Long Wave Model

Introduction

The importance of long equatorial waves in the development of El Niño has been widely recognized since the seminal works of Wyrtki (1975) and McCreary (1976). Equatorial-ocean linear models, forced by observed winds, have been quite successful in reproducing the major sea-level signature of El Niño (see, e.g., Busalacchi *et al.*, 1983). This event is the result of an intrinsic coupling between tropical ocean and atmosphere (El Niño-Southern Oscillation, or ENSO), and both simple and complex coupled ocean-atmosphere models have been developed to understand the phenomenon (McCreary and Anderson, 1991; Neelin *et al.*, 1992). Analyses of model solutions have led to several interesting ENSO theories, such as the delayed-action oscillator (Suarez and Schopf, 1988; Battisti and Hirst, 1989), in which equatorial Rossby and reflected Kelvin waves are important. Unstable coupled ocean-atmosphere modes therefore may be at the origin of ENSO. According to Wakata and Sarachik (1991), these modes are sensitive to the choice of Rayleigh friction.

Dissipation in the form of Rayleigh friction was introduced by Gill (1980) in an equatorial long-wave model. For a multiple-mode linear model, friction is usually taken as a vertical-mode dependent parameter (if possible based on physical assumptions) to allow separation into vertical modes (McCreary, 1981). Gent *et al.* (1983) discuss the equivalence of horizontal and vertical damping with Rayleigh friction and its vertical-mode dependence. Through a model best fit of the observed semiannual zonal current oscillation in the equatorial Indian Ocean, the same authors found a first-vertical-mode decay time of two years. Without a better estimate of damping, many modelers have used a similar value for the Rayleigh-friction coefficient.

The purpose of our study is to estimate the Rayleigh-friction coefficient in an equatorial long-wave model, constraining sea-level results to best fit three independent observed sea-level data sets (tide gauges, moorings and GEOSAT). Following the results of Busalacchi and Cane (1985), where the addition of the third and fourth vertical modes does not add any constructive information to their model/data intercomparison, our study is done using two vertical modes, and without any *a priori* hypothesis on the dependence of the friction coefficient on mode number.

Data

The longest sea-level data set (1975-89) used in this study is deduced from daily means of tide-gauge measurements at 14 islands, situated mostly in the western Pacific (Figure 1). Between instrumental uncertainties, island and barometric effects, the error in sea-level estimates is of the order of a few centimeters.

Daily mean, surface dynamic-height fields, relative to 500 db, are derived from the temperature sensors of nine TOGA-TAO moorings and three current meter moorings (McPhaden and Hayes, 1990), using Levitus (1982) mean TS relations. Most of the dynamic-height time series cover the 1986-91 period, except at 0°-140°W and 0°-110°W, where they start in November 1983. The significance of these open-ocean time series is altered by several gaps and technical constraints (such as the use of a reference level, mean TS relations, and inadequate vertical temperature sampling), which probably result in error ranges at least equal to those of the tide-gauge measurements.

The GEOSAT altimetric sea-level data, resulting from the geodetic and exact-repeat missions, cover the April 1985 - October 1989 period over most of the tropical Pacific (Figure 1). There is a gap in the data from 30 September 1986 to 8 November 1986 between the two different missions, and there is serious data degradation after May 1989. This data set was built on a 8° longitude x 1° latitude grid and interpolated to daily values. Detailed information about data combination within the two missions, their corrections, and their processing can be found in Miller and Cheney (1990) and Cheney *et al.* (1991a). The improved water-vapor and orbit corrections result in an rms difference between monthly GEOSAT and island sea level of 3 to 4 cm (Cheney *et al.*, 1991b).

TOGA Notes

Nova University
Oceanographic Center
8000 North Ocean Drive
Dania, Florida 33004, USA

JANUARY 1993

TOGA Notes

TOGA Notes is published quarterly by the Nova University Press. Its purpose is to provide a forum for presenting to the scientific community in a timely way new theories and findings on TOGA-related issues. Contributions will be published without charge and will not be copyrighted. Articles will be reviewed by the Science Editor, **Dr. Julian P. McCreary**, but, in the interest of time, will not be sent to outside referees for review. Most manuscripts will not be returned to authors for revision, provided that the articles are complete and otherwise suitable for publication. Permission to use scientific material contained in this bulletin must be obtained from the authors.

Manuscripts should be double-spaced, and figures must be camera-ready and suitable for reduction. References should be in the style of JAS/JPO and should be accurate, up-to-date, and complete. It should be noted that editors of refereed journals usually require that citations of bulletin articles be referenced as Personal Communication. A properly identified 5.25" floppy diskette (CP/M or MS-DOS), preferably in ASCII format, may accompany the manuscript. Authors are asked to provide complete mailing addresses; telephone, Fax, and Telex numbers; and E-mail addresses.

Manuscripts received within 6 weeks of a publication date, if accepted, will be included in that issue. Manuscripts should be submitted to the following address:

Ms. Jan Witte, Technical Editor
TOGA Notes
Nova University Oceanographic Center
8000 North Ocean Drive
Dania, Florida 33004, U.S.A.

Phone: (305) 920-1909; Fax: 947-8559
E-Mail (Omnet): J.McCreary or J.Witte

Items concerning International TOGA Project Office (ITPO) planning or announcements should be sent to:

Mr. John Marsh, Director
ITPO, c/o WMO
Postal Box 2300
CH-1211 Geneva 2, Switzerland

Phone: 41 22 7308 225 (Director)
Fax: 41 22 734 23 26; Telex: 23260
E-Mail (Omnet): INTL.TOGA or V.Lee

CONTENTS